

## THE IRRADIATION-INDUCED OLIVINE TO AMORPHOUS PYROXENE TRANSFORMATION PRESERVED IN AN INTERPLANETARY DUST PARTICLE

FRANS J. M. RIETMEIJER

Department of Earth and Planetary Sciences, MSC 03-2040, 1-University of New Mexico, Albuquerque, NM 87131-0001, USA; [fransjmr@unm.edu](mailto:fransjmr@unm.edu)  
Received 2009 July 2; accepted 2009 September 20; published 2009 October 15

### ABSTRACT

Amorphization of crystalline olivine to glass with a pyroxene composition is well known from high-energy irradiation experiments. This report is on the first natural occurrence of this process preserved in a chondritic aggregate interplanetary dust particle. The Fe-rich olivine grain textures and compositions and the glass grain compositions delineate this transformation that yielded glass with Fe-rich pyroxene compositions. The average glass composition,  $(\text{Mg}, \text{Fe})_3\text{Si}_2\text{O}_7$ , is a serpentine-dehydroxylate with  $\text{O}/\text{Si} = 3.56 \pm 0.25$ ,  $(\text{Mg}+\text{Fe})/\text{Si} = 1.53 \pm 0.24$ , and  $\text{Mg}/(\text{Mg}+\text{Fe}) = 0.74 \pm 0.1$ . These measured atomic ratios match the ratios that have been proposed for amorphous interstellar silicate grains very well, albeit the measured  $\text{Mg}/(\text{Mg}+\text{Fe})$  ratio is lower than was proposed for amorphous interstellar silicate grains,  $\text{Mg}/(\text{Mg}+\text{Fe}) > 0.9$ .

*Key words:* comets: general – dust, extinction – ISM: abundances – methods: laboratory

### 1. INTRODUCTION

Crystalline silicates entering the interstellar medium (ISM) find themselves in an environment that is conducive to destruction of their crystalline nature by grain–grain collisions, gas–grain collisions, interactions with photons and cosmic rays, or in multiple supernova shock waves where it may cause the emergence of amorphous silicates (Seab & Shull 1986; Demyk et al. 2001; Molster & Waters 2003; Molster & Kemper 2005). The energies in such shock waves can be simulated by irradiation experiments using  $\text{He}^+$ ,  $\text{H}^+$ , and  $\text{Ar}^{++}$  ions that will be effective for grains of about one micron or smaller in size (Carrez et al. 2001, 2002a; Demyk et al. 2001; Jäger et al. 2003; Brucato et al. 2004). The composition of the amorphous interstellar silicate grains remains uncertain. Westphal & Bradley (2004, p. 1140) noted, “The absence of average interstellar dust—amorphous silicates with bulk chemistry consistent with ISM gas-phase depletion—in IDPs is unexplained.” These interplanetary dust particles (IDPs) have a matrix that consists of  $<500$  nm amorphous silicate grains (Rietmeijer 1998, 2002) that include GEMS, glass with embedded metals, and sulfides (Bradley 1994). Bradley & Ishii (2008) hypothesized that interstellar silicates following irradiation-induced amorphization survived as GEMS in IDPs but this notion is not universally accepted (Martin 1995; Min et al. 2007).

A small fraction of silicate dust in disks around evolved stars is “crystalline silicate” of mostly olivine ( $(\text{Mg}, \text{Fe})_2\text{SiO}_4$ ) with lesser enstatite ( $\text{Mg}_2\text{Si}_2\text{O}_6$ ) and the Ca-rich pyroxene diopside ( $\text{CaMgSi}_2\text{O}_6$ ) with the remainder as amorphous silicates (Molster & Waters 2003; Molster & Kemper 2005). Astronomers using infrared (IR) spectroscopy report “crystalline silicate” but Earth scientists use the appropriate mineral names, e.g., olivine with an ordered crystal structure and a unique stoichiometric composition that ranges from  $\text{Mg}_2\text{SiO}_4$  (forsterite; Fo) to  $\text{Fe}_2\text{SiO}_4$  (fayalite; Fa). To Earth scientists, the astronomical “amorphous silicate” is an amorphous phase with an olivine composition.

Amorphization of minerals is a well-studied physical process. Irradiation will initially mobilize crystallographic imperfections (e.g., lattice vacancies) causing very small voids (pores) that are stabilized by the irradiating gas atoms and typically aligned on

crystallographic planes or grain boundaries (Hobbs et al. 1994). Such irradiation-induced voids are present in Fe-rich rims on isolated, micrometer scale, forsterite ( $\text{Fo}_{100-85}$ ) in the matrix of carbonaceous meteorites (Akai 1994; Tanaka & Akai 1997). Crystallographically oriented voids are present in a narrow ( $\sim 45$  nm) rim on an Mg-rich forsterite in the partially melted matrix of a cometary IDP (Rietmeijer 1996) that was captured in the Earth’s lower stratosphere (Mackinnon et al. 1982; Brownlee 1985; Warren & Zolensky 1994; Rietmeijer 1998). Rather than tracing complete amorphization, ultra-high vacuum  $\text{H}^+$  and  $\text{He}^+$  irradiations traced the formation of an amorphous glass rim on San Carlos olivine that is Fe-enriched and Mg-depleted relative to the underlying olivine grain and wherein  $\text{Fe}^{2+}$  in olivine was reduced to  $\text{Fe}^0$  forming nanometer size metal precipitates in the rim (Bradley et al. 1996). Rims with similar radiation fingerprints were found on olivine, Fe-sulfide, Fe-metal, and AlSiO-glass grains that were relic grains inside GEMS in several IDPs (Bradley et al. 1998; Westphal & Bradley 2004).

Continued irradiation using higher fluences or higher energies causes amorphous domains in the crystal lattice and ultimately complete amorphization (Wang & Ewing 1992a; Wang et al. 1993). Low-energy He ion irradiation changed the structure and chemical composition in crystal grains of San Carlos olivine,  $\text{Mg}_{1.8}\text{Fe}_{0.2}\text{SiO}_4$ , which is a standard frequently used in experiments. The changes included (1) increasing void size and density, (2) the non-equilibrium phase transformation of olivine to nanometer scale MgO crystals and  $\text{SiO}_2$ -rich glass, (3) O and Mg loss with increasing fluences ( $\text{He cm}^{-2}$ ), and (4) complete transformation to stoichiometric pyroxene glass with atomic ratios  $\text{O}/\text{Si} = 3$  and  $\text{Mg}/\text{Si} = 1$  (Carrez et al. 2001, 2002a; Demyk et al. 2001).

A comparative study of ion-beam irradiation induced amorphization in different silicates found that the Si–O covalent bonds of silicate structures are “weakest link” in this process (Eby et al. 1992). The susceptibility to ion beam-induced amorphization of a silicate mineral correlates with its glass-forming ability: the greater the glass-forming ability, the easier it will become amorphous (Wang et al. 1998a). As such pure forsterite is resistant to amorphization. The susceptibility to irradiation-induced amorphization is expressed by the theoretically derived relationship,  $T_m - T_c = K/S_0$ , wherein  $T_c$  is the critical

amorphization temperature,  $T_m$  the melting temperature,  $K$  is a constant specific to irradiation conditions, and  $S_0$  is the susceptibility to amorphization of a material (Wang et al. 1998b). This relationship predicts that fayalite is more susceptible to amorphization than forsterite (Wang & Ewing 1992b; Wang et al. 1998a, 1998b, 2001), especially at temperatures of  $\sim 700$ – $873$  K (Wang et al. 1995).

I report here the natural irradiation-induced transformation of olivine to “amorphous pyroxene” in chondritic aggregate IDP L2011K7 captured in the Earth’s lower stratosphere. This aggregate IDP is a remnant of the 4.56 Ga old dust that accreted in the solar nebula. The stoichiometric diopside pyroxene in this IDP contains irradiation-induced vesicles and lattice defects (i.e., solar flare tracks) and shows loss of O, Mg, and Ca+Mg. Most diopside grains were transformed into glass with either non-stoichiometric Mg-wollastonite pyroxene compositions or highly vesicular amoeboid glass with a (Si-rich) smectite composition (Rietmeijer 1999). For no other reason than close association of Mg, Fe-olivine grains in the same aggregate IDP L2011K7, they too were exposed to the same irradiation environment that caused the irradiation-induced transformation of Mg, Fe-olivine minerals to amorphous pyroxene. In this paper, I will use glass instead of amorphous solid in order to maintain a connection to the GEMS terminology and not concern myself with the degree of disorder of the amorphous phases.

## 2. EXPERIMENTAL TECHNIQUES

Particle L2011K7 was embedded in epoxy (Spurrs) at the NASA Johnson Space Center Curatorial Facility. Serial sections were prepared using a Reichert–Jung Ultramicrotome E in the Electron Microbeam Analysis Facility at UNM, where all analyses were conducted. Several ultra-thin (90 nm) sections were placed on holey a carbon thin-film that was supported on a standard 200 mesh Cu grid for study in a JEOL 2000FX AEM. Individual grids were housed in a Gatan low-background, double-tilt specimen holder for analysis using a JEOL 2000FX Analytical and Transmission Electron Microscope (ATEM). ATEM was operated at an accelerating voltage of 200 keV and was equipped with a Tracor-Northern TN-5500 energy dispersive spectrometer (EDS) for in situ analysis of elements  $>11$  atomic number using a 15 nm probe size. Quantitative data were obtained using the Cliff & Lorimer (1975) thin-film correction procedure and experimentally determined  $k$ -factors on natural standards (Mackinnon & Kaser 1987). The error in abundances of major-element oxides is 5% relative. The data reduction program calculated atomic abundances assuming compositional stoichiometry with iron as FeO. It is a normal procedure. Care was taken to ensure that the EDS probe only included a grain of interest. The probe size and beam current were monitored during EDS analyses to ensure reproducible conditions. To determine its thickness, the grain was imaged at two different tilt angles. The data are artifact free. To test the accuracy and precision of the EDS analyses, a powder sample of a diopside standard was prepared for AEM analyses in the same manner as the IDP. Ultrathin sections of the standard were analyzed under the same experimental conditions. Standard selected area electron diffraction analyses were used to determine the crystallographic grain properties, i.e., a crystalline (mineral) or amorphous (glass) solid. Diffraction patterns of crystalline materials show an ordered pattern of a single crystal mineral or rings of diffraction maxima for a polycrystalline mineral grain. A diffuse ring pattern without diffraction maxima indicates an amorphous solid.

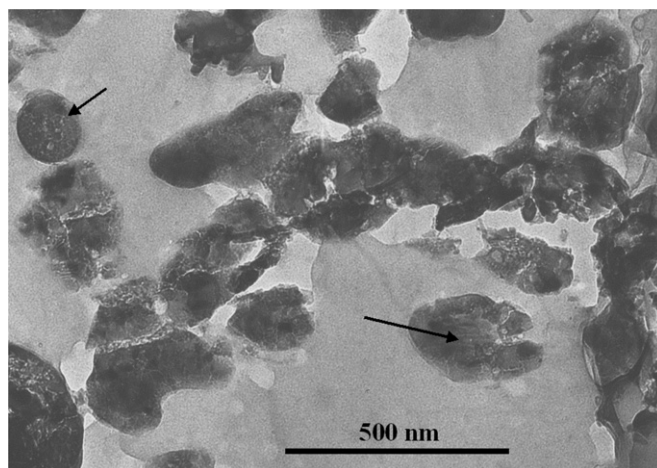


**Figure 1.** Transmission electron image of an ultrathin section cut from IDP L2011K7 showing, in the lower right-hand part (arrow), an olivine core (arrow) with an amorphous silicate rim (cf. Figure 4, arrow 1) and, in the upper left-hand corner (arrow), a rounded glass grain with small vesicles with a Mg, Fe-pyroxene composition. The other grains in this image show various stages in the irradiation-induced transformation of (crystalline) olivine to glasses with a pyroxene composition.

## 3. OBSERVATIONS

### 3.1. Petrographic Properties

The very low sulfur IDP L2011K7,  $22 \times 17 \mu\text{m}$  in cross section, is dominated by areas of highly vesicular, mostly ferromagnesian silica glass and elongated and rounded (spherical) grains of the same materials. Clusters of rounded grains (100–200 nm in size) are generally somewhat porous and enclose micrometer-scale minerals and silica-rich glass. The minerals are diopside and its irradiation-induced transformation products (Rietmeijer 1999), Mg, Fe-olivine, rare enstatite ( $\text{Mg}_2\text{Si}_2\text{O}_6$ ), and rare Ni-bearing (6 at% Ni) pyrrhotite. Olivine grains, and glass grains with pyroxene compositions and compositions intermediate between olivine and pyroxene (see below), range from 190 nm to 435 nm in diameter for spherical grains. These grains forming flattened spheroids (aspect ratios of  $\sim 0.5$ ) range from  $280 \text{ nm} \times 135 \text{ nm}$  to  $1060 \text{ nm} \times 615 \text{ nm}$ . Most of these grains are between 270 nm in diameter (spheres) and  $275 \text{ nm} \times 136 \text{ nm}$  in size. They occur as individual grains or in small clusters, and it is possible that the largest glass grains are fused clusters. Very few olivine grains still show their characteristic external shape. The trend is toward rounding off of grain edges and ultimately spherical and flattened spherical grains. Few grains have core of a remnant olivine grain. Typical grains have a smooth amorphous core, which often contains small ( $\sim 5$  nm to  $\sim 15$  nm), rounded relict grains, that gradually changes into a mélange of fine-grained glass grains, small crystals and many voids (pores), typically a few nanometers in size but up to 10–20 nm sized vesicles (Figure 1). These changes in petrographic properties are consistent with the gradual transformation of Fe-rich olivine mineral grains to glass grains with pyroxene compositions caused by irradiation-induced amorphization.

### 3.2. Olivine Amorphization Chemistry

The mean (at)  $\pm$ S.D. major abundances for all olivine and pyroxene glass compositions define Gaussian, distributions for  $\text{Si} = 17.2 \pm 4.5$ ,  $\text{Fe} = 6.7 \pm 3.85$ , except  $\text{Mg} = 16.65 \pm 6.4$  that shows a skewed ( $S$ ) distribution (mode = 19.11;  $S = -0.38$ ) indicating the grains are dominated by high Mg compositions.

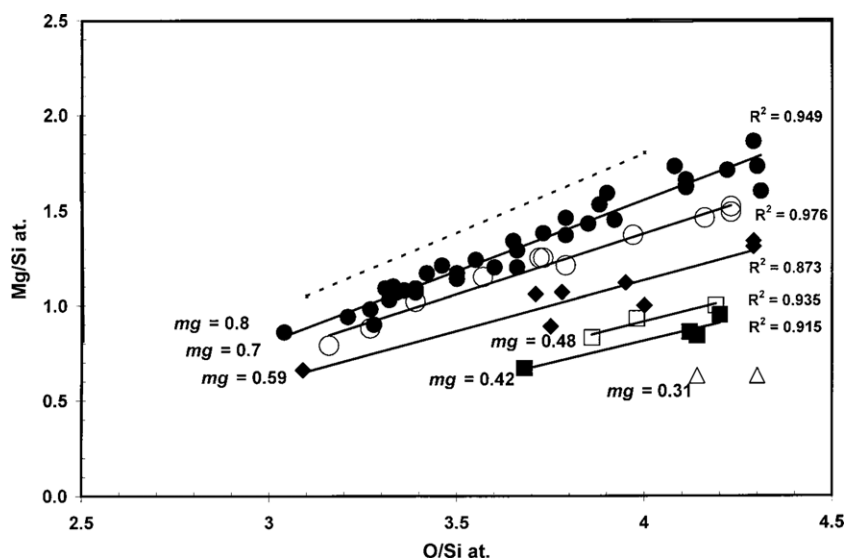


**Figure 2.** Linear correlations between the Mg/Si and O/Si ratios as a function of *mg* groups (dots, open circles and solid diamonds) of the natural transformation of crystalline olivine to stoichiometric pyroxene glass in IDP L2011K7 (solid lines) and their correlation coefficients. For comparison, the figure shows the correlation for the irradiation-induced transformation of olivine,  $\text{Mg}_{1.8}\text{Fe}_{0.2}\text{SiO}_4$  ( $mg = 0.9$ ; Carrez et al. 2002a; dotted line). In this experimental study, the O/Si (at) ratio decreased from 4 to 3 and the Mg/Si (at) ratio decreased from 1.8 to 1 (Carrez et al. 2002a).

**Table 1**

Range, Mean (atomic), and Standard Deviations (in parentheses) of Olivine and Glass Grains in IDP L2011K7 Ordered by *mg*-Ratio Groups

<i>mg</i> Ratio Groups		
Group	Range	Mean; <i>N</i>
0.80	0.86–0.75	0.80(0.03); 35
0.70	0.74–0.65	0.70(0.02); 11
0.59	0.64–0.55	0.59(0.02); 8
0.48	0.54–0.45	0.48(0.04); 3
0.42	0.44–0.35	0.42(0.02); 4
0.31	0.31–0.31	0.31; 2

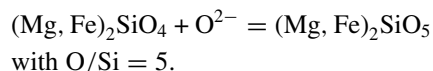
**Note.** *N* is the number of individual grains.

The average atomic Mg/(Mg+Fe) (*mg*) ratio,  $mg = 0.71$ , shows that the grains in this IDP are Fe-rich. The data are ordered in discrete size bins according to the Mg contents expressed as the *mg* ratio. It allows tracking of any effects that could be related to the differential susceptibility of olivine minerals, i.e., the fayalite ( $\text{Fe}_2\text{SiO}_4$ ) component of the grains being more susceptible to amorphization than forsterite ( $\text{Mg}_2\text{SiO}_4$ ). The olivine crystals in the irradiation study by Carrez et al. (2002a) contained a lower amount of iron, viz.,  $mg = 0.9$ .

The full range of olivine and glass grains in IDP L2011K7 ranges from  $mg = 0.80$  to  $mg = 0.31$  (Table 1). Few olivine and pyroxene glass grains have a pure Mg, Fe-composition. Most contain heterogeneously distributed, minor amounts of Al ( $\mu = 1.0 \pm 0.7$  at %) or Ni ( $\mu = 0.08 \pm 0.07$  at %), or both. The amount of Al increases slightly from olivine to stoichiometric pyroxene glass. These low contents will not affect the olivine susceptibility to amorphization (Wang et al. 1998a, 1998b). Iron and nickel will behave in a similar manner in silicates. It is not anticipated that these low Ni contents will affect the amorphization process. These low Al and Ni contents are normal for olivine and Ca-free pyroxene in IDPs (Rietmeijer 1998).

The co-linear decreases in the O/Si and Mg/Si ratios in low-energy helium irradiation experiments (Carrez et al. 2002a) imply stoichiometric Mg and O loss during the transformation of olivine to amorphous pyroxene. The data sets for the

*mg* groups 0.8, 0.7, and 0.59 (Table 1) are large enough to draw meaningful conclusions. Only eight grains represent the *mg* groups 0.48, 0.42, and 0.31. The data for the olivine to pyroxene glass transformation are shown in two complementary diagrams, viz. Mg/Si versus O/Si (at) (Figure 2) and Fe/Si versus O/Si (at) (Figure 3). The observed Mg/Si versus O/Si correlations conform to the experimentally determined trend (cf. Carrez et al. 2002a). In olivine, the stoichiometric O/Si (at) = 4, in stoichiometric pyroxene O/Si (at) = 3. Olivine in the  $mg = 0.8$  group with a smooth grain surface, i.e., no discernable irradiation-induced voids, include two different O/Si populations, viz., (1) O/Si =  $4.09 \pm 0.17$ , i.e., statistically stoichiometric olivine and (2) O/Si =  $4.28 \pm 0.04$ . The latter matches the solar ratio, O/Si = 4.32, which seems coincidental. Similar high O/Si ratios for GEMS (Table 2) were explained as excess oxygen due to the amorphization process, although no complete explanation was offered. In IDP L2011K7, excess oxygen occurs in Fe-rich, crystalline olivine, and thus from a mineralogical point of view the reaction may have been of the type



Oxidation of a fraction of ferrous iron in the fayalite component of olivine could introduce excess oxygen, viz.  $^{2+}\text{Fe}_{2-x}^{3+}\text{Fe}_x\text{SiO}_{4+0.5x}$  with  $x \leq 1$ . The observed average O/Si ratio of 4.28 suggests that 30% of the fayalite component was stoichiometric  $^{2+}\text{Fe}_{1.4}^{3+}\text{Fe}_{0.6}\text{SiO}_{4.3}$  but with excess oxygen. If this oxidation reaction is an accurate explanation for this excess oxygen in Fe-rich olivine in this IDP, the cause for this unusual mineralogical reaction must also be unusual. Irradiation-induced olivine amorphization qualifies as an unusual mineralogical process.

The sequence of events that resulted in natural samples for laboratory analyses is often difficult to unravel, such as variations in oxidation/reduction conditions during amorphization of Fe-rich olivine. Following the original amorphization process several different and independent processes might have affected

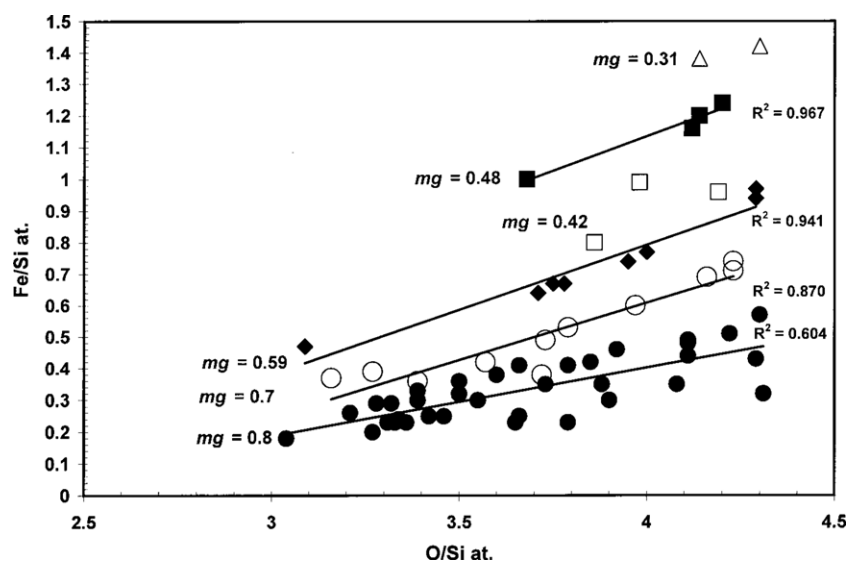


**Figure 3.** Fe/Si and O/Si ratios separated by *mg* group (dots, open circles, and solid diamonds) and linear correlation coefficients for the same grains as in Figure 2.

**Table 2**

The Values of Defining Parameters of Amorphous Interstellar Silicate Grains and These Values for GEMS in IDPs are Compared to Glass Grains Due to the Olivine–Pyroxene Glass Transformation

Mg/(Mg+Fe) (mg)	(Mg+Fe)/Si	O/Si	References
Astronomical observation			
>0.9	≈1.5	≈3.5	#1
GEMS in chondritic aggregate IDPs			
No data	≈0.7	≈2.7	#2
0.24–0.84	0.48–1.99	3.93–4.22	#3
0.60 (0.18)	1.05 (0.49)	3.98 (0.59)	#4
0.59	1.09	4.35	#5
Olivine–pyroxene glass transformation (this study)			
0.74 (0.1)	1.53 (0.24)	3.56 (0.25)	#6

**Notes.** The mean values or range are presented; the S.D. is shown in parentheses. The mean and standard deviation were calculated by the author.

**References.** #1: Min et al. 2007; #2: Keller & Messenger 2004; #3: Bradley 1994; #4: Bradley & Ireland 1996; #5: Ishii et al. 2008; #6: this work.

the mineral and glass grains in this IDP, viz., (1) dynamic annealing of the fayalite component in olivine during irradiation at elevated temperatures ( $\sim 600^\circ\text{C}$ ) causing nucleation (crystallization) of quartz ( $\text{SiO}_2$ ) and magnetite ( $\text{Fe}_3\text{O}_4$ ) nanocrystals in amorphized material (Wang et al. 1995), (2) oxidation caused by flash-heating of the grains in this IDP the few seconds of during atmospheric entry up to  $\sim 600^\circ\text{C}$  (Rietmeijer 1999) or both. The low Fe/Si versus O/Si linear correlation coefficient (0.6) of the *mg* = 0.8 group (Figure 3) might point to the actions of untraceable oxidation/reduction conditions, or it simply shows a larger error of measurement in this very low-Fe glass.

### 3.3. Chemical Zoning

Many grains have a core-rim texture whereby the core has a (relict) olivine composition. Selected core-rim examples are shown in Figure 4. In general, the compositions of the amorphous rims in most show a trend toward higher silica ( $\text{SiO}_2$ ) contents, that is, glass with (1) a smectite dehydroxylate composition or (2) pyroxene composition (Figure 4; arrows 1 & 2). In only one zoned grain the olivine core has an amorphous pyroxene rim that is more Mg-rich than the core suggesting the loss of Fe and O (Figure 4; arrow 3). This trend is consistent with heating olivine to temperatures close

to its melting point. It is an anomaly among the data that might indicate another process than irradiation-induced amorphization or a secondary process that affected the most Fe-rich olivine in this IDP. In two other grains the rim was pure silica glass on a smectite dehydroxylate core (no relict olivine) or pure silica glass on pyroxene glass with a small relict olivine core (Figure 4, arrows 4). They were the two smallest grains in IDP L2011K7, which suggests that irradiation-induced element loss is volume diffusion-controlled. The smectite dehydroxylate (see below) composition suggests kinetically control on the irradiation-induced amorphization process in this IDP.

## 4. DISCUSSION AND CONCLUSIONS

A previous study of diopside in this IDP showed how energetic ion bombardment created (Ca, Mg)O vacancies in diopside crystals that ultimately led to its amorphization and the formation of Mg, Ca-silica glass (Rietmeijer 1999). The present study documented the continuous amorphization of crystalline Mg, Fe-olivine to glass with a stoichiometric pyroxene composition that had occurred naturally and was preserved in the interplanetary dust particle L2011K7. The olivine grains have wide range of compositions from *mg* = 0.80 to *mg* = 0.31. The high iron contents could have facilitated the amorphization

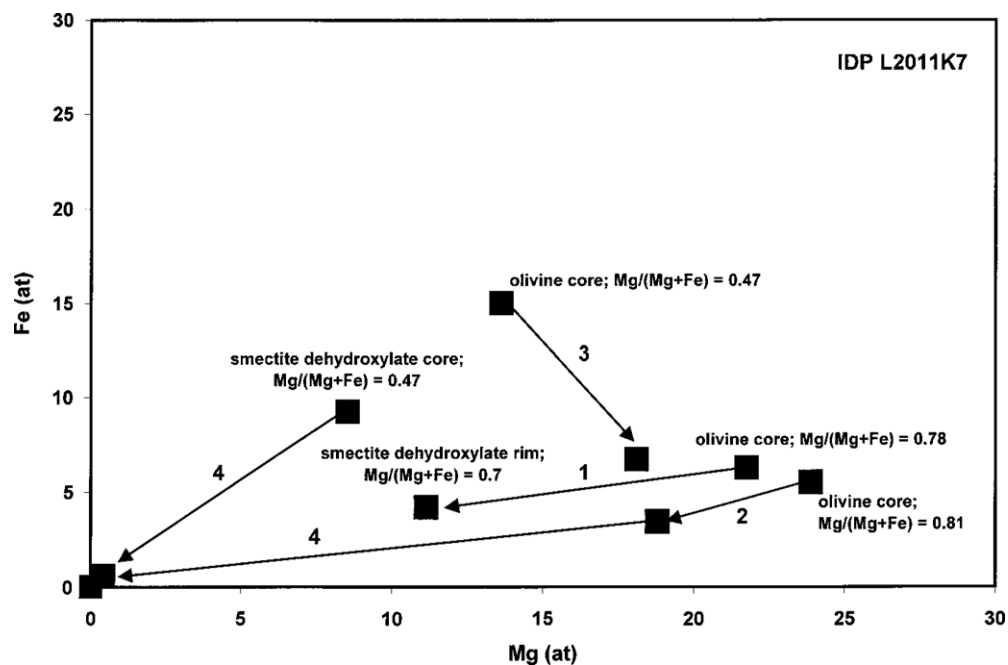


**Figure 4.** Selected examples of compositionally zoned grains due to the irradiation-induced olivine-pyroxene transformation preserved in aggregate IDP L2011K7: (1) a crystalline olivine core and smectite dehydroxylate composition rim (most common), (2) a crystalline olivine core and pyroxene composition glass rim, (3) (extremely rare) olivine core with an amorphous pyroxene rim more Mg-rich than the core, and (4) a rare grain with a pure silica glass rim on a smectite dehydroxylate core (no relict olivine), and an outer silica glass rim on pyroxene glass still with a small relict olivine core

process. Fayalite amorphization displays anomalous behavior that can be linked to the iron oxidation state whereby  $\text{Fe}^{3+}$  dramatically increases its susceptibility to amorphization (Wang et al. 1998b). The resulting glass will have Fe-bearing to Fe-rich pyroxene compositions. Depending on the *mg* ratio of olivine, and whether Fe-loss during amorphization was stoichiometric (this study) or not (Carrez et al. 2002a), this process should yield (Mg, Fe)O molecules or dust with variable compositions that were detected around protostars but not, yet, in the interstellar medium (Molster & Waters 2003). However, thermal treatment of fully amorphized materials in the laboratory often induced the nucleation and rapid formation of non-equilibrium nanometer scale minerals (Carrez et al. 2002b; Wang et al. 1995).

#### 4.1. Amorphous Interstellar Silicate Grains?

The solar system sources of chondritic aggregate IDPs remain unknown but since their textures and petrological properties are entirely different from these properties of any meteorites in our collections, they are from small solar system bodies that are not parent bodies of these meteorites (Mackinnon & Rietmeijer 1987). It suggests a cometary reservoir for these particles. If this connection can be made, IDP L2011K7 accreted from dust that was modified prior to the accretion of comets. Once accreted in a comet nucleus, this IDP and its constituents were preserved in their original mineralogical state that may have included amorphous interstellar silicate grains and silicates that were modified by irradiation-induced amorphization in the solar nebula.

Min et al. (2007) modeling the shape and compositions of amorphous interstellar silicate grains concluded that these silicates are on average Mg rich (*mg* > 0.9). The defining parameters in this model (Min et al. 2007) are well matched by those for the average amorphous silicates in IDP L2011K7 here reported (Table 2). The average *mg* ratio is smaller than the value in the model of Min et al. (2007) but observed compositions in the IDP silicates are dominated by high-Mg compositions. The

data presented in a O/Si versus (Mg+Fe)/Si (at) diagram show that the composition of the amorphous interstellar silicate (cf. Min et al. 2007) perfectly matches a serpentine-dehydroxylate,  $(\text{Mg, Fe})_3\text{Si}_2\text{O}_7$ , composition for the average glass composition in IDP L2011A9 (Figure 5). The most Si-rich glass composition observed in this IDP matches a smectite-dehydroxylate,  $(\text{Mg, Fe})_6\text{Si}_8\text{O}_{22}$ , composition (Figure 5). These two particular compositions point to a lack of thermodynamic equilibrium during the olivine amorphization process. Highly disordered amorphous solids with these deep metastable eutectic compositions formed preferentially in vapor phase condensation experiments (Nuth et al. 2000a; 2000b; Rietmeijer et al. 2002) and they match many of the compositions of glass grains in chondritic aggregate IDPs (Rietmeijer 2002; Rietmeijer et al. 1999). The physiochemical conditions necessary to form these metastable dehydroxylate glasses are rapid quenching to well below its solidus of a super-heated melt or a vapor. How exactly these conditions can be connected to high-energy induced amorphization of silicates is not yet clear but I recall that the susceptibility to amorphization of silicates was linked to their glass-forming ability. Studies of irradiation-induced amorphization showed that amorphization of pure forsterite is much more difficult to achieve than for Fe-containing olivine minerals (cf. Wang et al. 1998a, 1998b). Amorphization of 200 nm diameter forsterite grains in the interstellar medium during  $10^7$ – $10^8$  yr produces a negligible fraction of amorphous forsterite grains (Brucato et al. 2004). When crystalline forsterite were the precursor of the amorphous interstellar silicate discussed by Min et al. (2007), it places rigorous constraints on the energies and times available for the amorphization process. The data presented here suggest that the olivine grains entering the interstellar medium include pure forsterite and Fe-rich olivine minerals. The latter will readily succumb to amorphization, which yields a mixed population of crystalline forsterite and Fe-rich amorphous silicate (glass) grains, unless extreme conditions also produced forsterite glass. Amorphization will be sensitive to

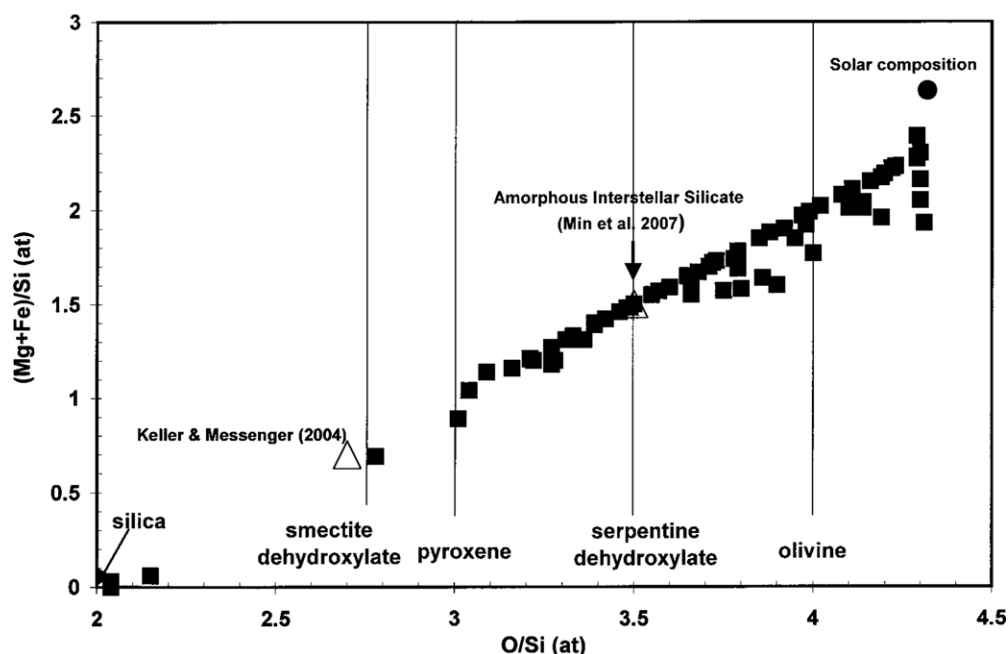


**Figure 5.** (Mg+Fe)/Si (at) vs. O/Si (at) diagram showing the olivine and glass compositions in IDP L2011K7 (solid squares), the amorphous interstellar silicate (open circle; source identified) and GEMS in IDPs (open triangle; source identified).

grain size that is also a sensitive parameter to reduce infrared spectroscopy data.

#### 4.2. Where are these Grains?

The compositions of the crystalline olivine to pyroxene glass transformation (Figure 5) are all for ~200 nm to ~1 micron, Fe-rich olivine mineral and glass grains with a wide range of *mg* ratios. Whether or not they are detectable using infrared spectroscopy is another matter. If these serpentine dehydroxylate glass grains are the amorphous interstellar silicate grains, it raises two questions: (1) could there be more than one type of interstellar silicate grains and (2) is the hypothesized GEMS interstellar silicate origin correct? It is not yet proven that all GEMS in the chondritic aggregate IDPs studied to date are pre-accretionally irradiated grains and could not include evolved non-equilibrium condensate grains (Rietmeijer 2009). There is no physical resemblance between GEMS and the dehydroxylate glass grains in IDP L2011K7 but both show the vesicular textures that developed in radiation-induced amorphization experiments. There are considerable chemical differences between GEMS and the amorphous interstellar silicate and the glass grains from this study (Table 2). It is remarkable then that the average O/Si ( $\approx 2.7$ ) and (Mg+Fe)/Si ( $\approx 0.7$ ) ratios for 144 GEMS (Keller & Messenger 2004) match the smectite-dehydroxylate glass composition in IDP L2011K7 (Figure 5). A possible scenario could be that interstellar Fe-rich ferromagnesian silicate grains from the crystalline olivine to pyroxene glass transformation continued to lose Mg with concomitant reduction of Fe and Ni from the silicate fraction to Fe, Ni-metal grains. The answer to these questions are then, yes, there are different types of amorphous silicate grains that formed by the process hypothesized for pre-accretionally irradiated GEMS. The chondritic aggregate IDP L2011K7 is the first primitive extraterrestrial sample that preserved evidence for the natural, irradiation-induced olivine to amorphous pyroxene transformation. If, as I hypothesize, the grains from this transformation represent amorphous interstellar silicate grains, then this metastable interstellar silicate has an

average Mg, Fe-serpentine-dehydroxylate composition with rare grains having a Mg, Fe-smectite dehydroxylate composition.

This paper has benefited from thoughtful review. This work was supported by grant NNX07AI39G from the NASA Cosmochemistry Program. All ATEM analyses were conducted in the Electron Microbeam Analysis Facility in the Department of Earth and Planetary Sciences at UNM.

#### REFERENCES

- Akai, J. 1994, Proc. NIPR Symp. Antarctic Meteorites, 7, 94  
Bradley, J. P. 1994, *Science*, 265, 925  
Bradley, J. P., Dukes, C., Baragiola, R., McFadden, L., Johnson, R. E., & Brownlee, D. E. 1996, *Lunar Planet. Sci.*, 27, 149  
Bradley, J. P., & Ireland, T. 1996, in ASP Conf. Ser. 104, Physics, Chemistry and Dynamics of Interplanetary Dust, ed. B. A. Gustafson & M. S. Hanner (San Francisco, CA: ASP), 275  
Bradley, J. P., & Ishii, H. A. 2008, *A&A*, 486, 781  
Bradley, J. P., Snow, T., Brownlee, D. E., Keller, L. P., Flynn, G. J., & Miller, M. 1998, *Lunar Planet. Sci.*, 29, 1737  
Brownlee, D. E. 1985, *Ann. Rev. Earth Planet. Sci.*, 13, 147  
Brucato, J. R., Strazzulla, G., Baratta, G., & Colangeli, L. 2004, *A&A*, 413, 395  
Carrez, Ph., Leroux, H., & Cordier, P. 2001, *Phil. Mag. A*, 81, 2823  
Carrez, Ph., Demyk, K., Cordier, P., Gengembre, L., Grimblot, J., d'Hendecourt, L., Jones, A. P., & Leroux, H. 2002a, *Meteorit. Planet. Sci.*, 37, 1599  
Carrez, Ph., Demyk, K., Leroux, H., Cordier, P., Jones, A. P., & d'Hendecourt, L. 2002b, *Meteorit. Planet. Sci.*, 37, 1615  
Cliff, G., & Lorimer, G. W. 1975, *J. Microscopy*, 103, 203  
Demyk, K., et al. 2001, *A&A*, 368, L38  
Eby, R. K., Ewing, R. C., & Birtcher, C. 1992, *J. Mat. Sci.*, 7, 3080  
Hobbs, L. W., Clinard, F. W., Jr., Zinkle, S. J., & Ewing, R. C. 1994, *J. Nucl. Mat.*, 216, 291  
Ishii, H. A., et al. 2008, *Science*, 319, 447  
Jäger, C. J., Fabian, D., Schrempel, F., Dorschner, J., Henning, Th., & Wesch, W. 2003, *A&A*, 401, 57  
Keller, L. P., & Messenger, S. 2004, *Lunar Planet. Sci.*, 35, 1985  
Mackinnon, I. D. R., & Kaser, S. A. 1987, in *Microbeam Analysis-1987*, ed. R. H. Geiss (San Francisco, CA: San Francisco Press), 332  
Mackinnon, I. D. R., & Rietmeijer, F. J. M. 1987, *Rev. Geophys.*, 25, 1527  
Mackinnon, I. D. R., McKay, D. S., Nace, G., & Isaacs, A. M. 1982, *J. Geophys. Res.*, 87, A413

- Martin, P. G. 1995, *ApJ*, **445**, L63
- Min, M., Waters, L. B. F. M., de Koter, A., Hovenier, J. W., Keller, L. P., & Markwick-Kemper, F. 2007, *A&A*, **462**, 667
- Molster, F. J., & Kemper, C. 2005, *Space Sci. Rev.*, **119**, 3
- Molster, F. J., & Waters, L. B. F. M. 2003, in *Lecture Notes in Physics*, Vol. 609, *Astromineralogy*, ed. Th. Henning (Heidelberg: Springer), 121
- Nuth, J. A., III, Hallenbeck, S. L., & Rietmeijer, F. J. M. 2000a, *J. Geophys. Res.*, **105**, 10387
- Nuth, J. A., III, Rietmeijer, F. J. M., Hallenbeck, S. L., Withey, P. A., & Ferguson, F. 2000b, in *ASP Conf. Ser. 196, Thermal Emission Spectroscopy and Analysis of Dust, Disks and Regoliths*, ed. M. L. Sitko, A. L. Sprague, & D. K. Lynch (San Francisco, CA: ASP), 313
- Rietmeijer, F. J. M. 1996, *Meteorit. Planet. Sci.*, **31**, 237
- Rietmeijer, F. J. M. 1998, in *Reviews in Mineralogy 36, Planetary Materials*, ed. J. J. Papike (Chantilly, VA: Min. Society of Amer.), 2
- Rietmeijer, F. J. M. 1999, *Am. Mineral.*, **84**, 1883
- Rietmeijer, F. J. M. 2002, *Chemie der Erde*, **62**, 1
- Rietmeijer, F. J. M. 2009, *Meteorit. Planet. Sci.*, **44**, 1121
- Rietmeijer, F. J. M., Nuth, J. A., III, & Karner, J. M. 1999, *ApJ*, **527**, 395
- Rietmeijer, F. J. M., Hallenbeck, S. L., Nuth, J. A., III, & Karner, J. M. 2002, *Icarus*, **156**, 269
- Seab, C. G., & Shull, J. M. 1986, in *NASA Conf. Publ. 2403, Interrelationships among Circumstellar, Interstellar, and Interplanetary Dust*, ed. J. A. Nuth & R. E. Stencel (Washington, DC: NASA), 37
- Tanaka, H., & Akai, J. 1997, *Antarct. Meteorit. Res.*, **10**, 217
- Wang, L. M., & Ewing, R. C. 1992a, *Mat. Res. Soc. Bull.*, **17**, 38
- Wang, L. M., & Ewing, R. C. 1992b, *Mat. Res. Soc. Proc.*, **235**, 333
- Wang, L. M., Miller, M. L., & Ewing, R. C. 1993, *Ultramicroscopy*, **51**, 339
- Wang, S. X., Wang, L. M., Ewing, R. C., & Doremus, R. H. 1998a, *J. Non-cryst. Solids*, **238**, 198
- Wang, L. M., Gong, W. L., Bordes, N., Ewing, R. C., & Fei, Y. 1995, *Mat. Res. Soc. Proc.*, **373**, 407
- Wang, S. X., Wang, L. M., Ewing, R. C., & Doremus, R. H. 1998b, *J. Non-cryst. Solids*, **238**, 214
- Wang, S. X., Wang, L. M., & Ewing, R. C. 2001, *Phys. Rev. B*, **63**, 024105
- Warren, J. L., & Zolensky, M. E. 1994, in *AIP Conf. Proc. 310, Analysis of Interplanetary Dust*, ed. M. E. Zolensky et al. (Melville, NY: AIP), 105
- Westphal, A. J., & Bradley, J. P. 2004, *ApJ*, **617**, 1131